Journal of Applied Fluid Mechanics, Vol. 16, No. 9, pp. 1717-1728, 2023.
Available online at www.jafmonline.net, ISSN 1735-3572, EISSN 1735-3645.
https://doi.org/10.47176/jafm.16.09.1840

Investigation of Flow Boiling in Micro-Channels: Heat Transfer, Pressure Drop and Evaluation of Existing Correlations

L. L. Feng[1], C. C. Cao[2], K. Zhong[1] and H. W. Jia[1†]

[1] *School of Environmental Science and Engineering, Donghua University, Shanghai 201620, China*
[2] *Shanghai Marine Diesel Engine Research Institute, Shanghai 201108, China*

†*Corresponding Author Email: jiahw@dhu.edu.cn*

ABSTRACT

In this study, the flow boiling heat transfer and pressure drop characteristics of refrigerant R134a in micro-channels were experimentally investigated. The tests were performed in circular horizontal micro-channels with inner diameters of 0.5 mm and 1 mm and a heating length of 300 mm. The mass velocities varied from 500 kg/m^{2}s to 2500 kg/m^{2}s, and the heat fluxes varied from 15 kW/m^2 to 147 kW/m^2. The heat transfer coefficient (HTC) and frictional pressure drop (FPD) were measured and discussed in detail. According to the results, HTC was significantly affected by heat flux, whereas it was independent of mass velocity. Nucleate boiling was the dominant heat transfer mechanism for R134a flow boiling in the micro-channels. In comparison to the 1 mm channel, the 0.5 mm channel shows better performance in heat transfer, with a maximum increase of approximately 22 %. In addition, FPD increased with increasing mass velocity and decreasing channel diameter. Finally, several existing correlations for HTC and FPD were evaluated by comparing them with the experimental values. Tran's correlation (1996) presented a better agreement in terms of the average HTC, while for the FPD, the model of Kim and Mudawar (2013b) showed good prediction accuracy.

Article History

Received February 20, 2023
Revised April 1, 2023
Accepted April 11, 2023
Available online July 1, 2023

Keywords:

Micro-channel
Flow boiling
Heat transfer
Frictional pressure drop
Predictive correlations

1. INTRODUCTION

Flow boiling is an extremely efficient form of heat dissipation that occurs frequently in practical applications, such as refrigeration, heat pumps, and air conditioning (A/C) and so on (Feng et al., 2022; Qiu et al., 2022). To improve the operating efficiency and heat transfer performance, many experimental investigations have been conducted using R-134a as the working refrigerant because of its wide range of applications and low cost.

For instance, Chen et al. (2021) performed subcooled flow boiling tests with narrow horizontal annuli and found that the HTCs for R-134a increased with the heat flux. Similarly, Saisorn et al. (2011) conducted a flow boiling experiment on R-134a in a horizontal channel with ID (inner diameter) =1.75 mm and found that the effect of heat flux on the HTC was remarkable, regardless of the mass velocity and vapor quality. Besides, in the study of Fayyadh et al. (2017), the HTC of R-134a in multi micro-channels was closely related to the heat flux, but the mass velocity effect was weak. Lee and Mudawar (2005) studied the HTC of R-134a in a compact heat sink with dimensions of 0.231 mm×0.713 mm. They concluded that nucleate boiling occurred only in the low-vaporquality regions corresponding to extremely low heat flux, whereas the evaporation of annular film was dominant at high heat flux, producing medium and high vapor quality. However, the experimental results on R-134a flow boiling in multi-port micro-channels with 1.1 mm and 1.2 mm IDs published by Kaew-On et al. (2011) indicated that nucleate boiling was the main mechanism for two-phase flow in the micro-channel. Recently, Dorao et al. (2018) systematically measured the HTC of R-134a in a 5 mm ID channel. It was found that the convective flow boiling HTC was equivalent to the single-phase convective flow HTC, and the effect of vapor velocity must be considered.

The diameter of the test channel has also been considered as an important parameter that affecting the boiling heat transfer (Gan et al., 1998). Kanizawa et al. (2016) studied the flow boiling characteristics in channels with IDs ranging from 0.38 to 2.6 mm, and found that the mass velocity, heat flux and saturation temperature could affect the HTC dramatically. However, the HTC decreased with an increase in the inner diameter. Saitoh et al. (2005) carried out tests on R-134a flow boiling in channels with various IDs from 0.51 mm to 3.10 mm.

Nomenclature

C	Chisholm parameter
D	channel diameter
f	friction factor
F	enhancement factor
FPD	frictional pressure drop
g	gravitational acceleration
G	mass velocity
h	heat transfer coefficient (HTC)
i	Enthalpy of the refrigerant
L	Channel length
m	mass flow rate
p	pressure
q	heat flux
Q	heat
S	suppression factor
T	temperature
x	vapor quality
X	Martinelli parameter
z	position along the channel

Greek symbols

ε	void fraction
ρ	density
λ	thermal conductivity
μ	viscosity
ϕ	two-phase multiplier
σ	Surface tension coefficient

Subscripts

a	acceleration
ave	average
conv	convective
exp	experimental
f	fluid
fric	friction
in	inner
l	liquid
nb	nucleate boiling
out	outer
pre	predicted
v	vapor

They found that nucleate boiling occurred only at low vapor qualities, whereas convective evaporation predominated under high vapor quality conditions. However, as the channel size decreased, the dominant role of convective evaporation diminished. In addition, the test results of Bertsch et al. (2009a) have concluded that the HTC was slightly increased with the mass velocity and kept almost constant in the 0.54 mm and 1.09 mm IDs of the micro-channel heat exchanger. Meanwhile, the heat exchanger with a smaller hydraulic diameter exhibited a slightly higher HTC. Wang and Sefiane (2012) investigated the influence of the channel size on the heat transfer in micro-channels. It was found that the effect of the channel size was more pronounced at high mass velocities, and the HTC decreased significantly with increasing channel diameter.

The process of phase change heat transfer in the micro-channel evaporator can lead to an apparent pressure drop, which is also an important parameter that related to the safe operation of the system. However, the pressure drop in micro-channel is not well understood. Experimental studies on pressure drop have been conducted. Xu et al. (2016) experimentally studied the FPD of R-134a in channels with IDs of 1.002, 2.168, and 4.065 mm. The experimental results indicated that the FPD initially increased with mass velocity and vapor quality, and then decreased with a further increase in vapor quality. Furthermore, a higher saturation temperature and larger hydraulic diameter can downgrade the FPD. Hwang and Kim (2006) also investigated the variation of FPD in micro-channels with IDs ranging from 0.244 mm to 0.792 mm. They found that increasing the vapor quality and mass velocity could increase the two-phase FPD, whereas increasing the channel diameter could reduce the FPD. However, the experimental values of the FPD deviated from the predicted values that calculated by the predictive models. In research on CO_2 flow boiling in a 1.42 mm micro-channel conducted by Wu et al. (2011), a higher mass velocity resulted in a higher FPD, but a higher saturation temperature resulted in a lower FPD, regardless of the heat flux contribution to the FPD. A similar result was obtained by Choi et al. (2008), in which the mass velocity and channel diameter significantly influenced the FPD of R-410A flow boiling in horizontal channels. Yang and Webb (1996) studied the FPD of R-12 flow boiling in a 2.64 mm rectangular plain channel and a 1.56 mm micro-fin channel. According to the results, the FPD increased as the mass velocity and vapor quality. Moreover, the micro-fin channel exhibited a significantly larger FPD than the plain channel under the same conditions. Dang et al. (2019) investigated the effect of continuous and segmented structures on the FPD in micro-channels using HFE-7000 as the working fluid. They found that the segmented micro-channel had a lower FPD than the continuous channel.

The present study aims to extend the knowledge of flow boiling heat transfer behaviors and characteristics in micro-channels, hence, the flow boiling of R-134a in 0.5 mm and 1 mm micro-channels was studied at mass velocities ranging from 500 kg/m^{2}s to 2500 kg/m^{2}s and heat fluxes from 15 kW/m^2 to 147 kW/m^2. The heat transfer and pressure drop characteristics were studied in detail, and the experimental results of the HTC and FPD were compared with the existing correlations, and the predictive performance was evaluated.

2. EXPERIMENTAL FACILITY AND DATA REDUCTION

2.1 Test Apparatus and Instrumentation

Figure 1 shows the schematic diagram of the test rig.

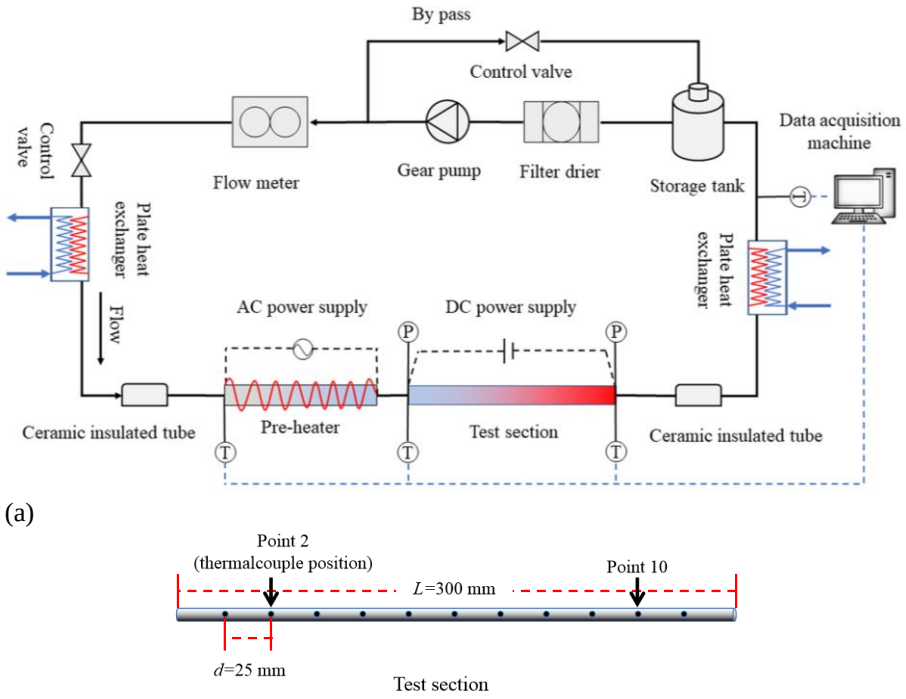

Fig. 1. Schematic of experimental test rig. (a) Test apparatus, (b) Test section.

The system consisted of two main circuits: a cooling loop and a refrigerant loop. The cooling loop used ethylene glycol solution as the coolant fluid and a low-temperature thermostatic bath as the cold source. Two plate heat exchangers were individually mounted before and after the test channel to cool the R-134a in the loop. The refrigerant loop includes a variable speed gear pump, a Coriolis-type mass flow gauge, an experimental section, a pre-heater, a condensation, a storage reservoir (SS304, 2 L), and a drying filter (DFS-052S-1/4, Hongsen). During the experiments, the subcooled liquid was fed into the experimental section by using a gear pump (GAFST23, Micropump). The mass velocity of the liquid was controlled by regulating the gear pump and was measured using a flow meter (DMF-1-1B). The preheater was wrapped in enamel-insulated heating wires and was heated using an AC power supply.

The test section was made of a 300 mm horizontal circular stainless-steel channel, as depicted in Fig. 1 (b). Two IDs of 0.5 mm and 1 mm were employed in the present study, and the diameters of both test channels were smaller than the critical diameter, following the definition of the micro-channel proposed by Kew and Cornwell (1997). Eleven equally spaced thermocouples (Points 1–11) were attached to the outer wall to measure the temperature along the flow orientation. Both ends of the test channel were fitted with sheathed thermocouples and pressure transducers to directly measure the temperature and pressure of the R-134a. Two copper electrodes were installed at each end of the channel and connected to a DC power source to heat the test channel. The test tube was covered with heat barrier material, and all devices were covered with 9 mm-thick insulating cotton with a heat conductivity coefficient of approximately 0.034 W/ m K to reduce the heat loss. Finally, all data were recorded by a data acquisition device (Agilent-34972A) every five seconds as steady state was reached and then stored in the computer.

Table 1 Uncertainty of experimental parameters.

Parameter	Uncertainty
Mass velocity, G (kg/m^{2}s)	±4.0 %
Heat flux, q (kW/m^2)	±2.12 %
Heat transfer coefficient, h (kW/m^{2}K)	±5.01 %
Vapor quality, x (-)	±0.87 %
Heat input, Q (W)	±0.71 %

Uncertainty analysis was performed for the experimental parameters using the method described by Moffat (1988). Based on the uncertainties of the measuring equipment listed in our previous study [2], the uncertainties of the derived parameters were calculated using Eq. (1), and the results are summarized in Table 1.

$$\delta R = \sqrt{\sum_{i=1}^{N}\left(\frac{\partial R}{\partial X_i}\delta X_i\right)^2} \tag{1}$$

2.2 Data Processing Method

The mass velocity G of the refrigerant in channel is defined as below:

$$G = \frac{4m}{\pi D_{in}^{\ 2}} \tag{2}$$

The heat flux q for heating the refrigerant is given as:

$$q = \frac{UI\eta}{\pi D_{in} L} \tag{3}$$

where η=0.789 represents the effective heating factor that is derived from the single-phase test.

The local HTC h_{local} is calculated by the equation below:

$$h_{local}(z)=\frac{q}{T_{wall,in}-T_{f,z}} \tag{4}$$

where $T_{wall,in}$ represents the wall temperature at the internal surface of the channel, and can be derived based on the one-dimensional Fourier's law.

$$T_{wall,in}=T_{wall,out}-\frac{qD_{in}\ln\left(D_{out}/D_{in}\right)}{2\lambda} \tag{5}$$

The local vapor quality x can be expressed as:

$$x(z)=\frac{\left(i_{l,in}-i_{sat}\right)+\varepsilon Qz/mL}{i_{l,v}} \tag{6}$$

More details regarding the test rig and data processing methods can be found in our previous study (Feng et al., 2022).

3. Results and Discussions

3.1 Boiling Curves

Figure 2 shows the boiling curves, i.e., the heat flux versus the wall superheat (T_{wall}-T_{sat}), of R-134a at four mass velocities from 1000 kg/m^{2}s to 2500 kg/m^{2}s in the 0.5 mm micro-channel. The experimental data at Point 2 and Point 10 were selected as examples. Two flow regimes are identified, as shown in Fig. 2. Regime I: the single-phase regime under lower heat flux (q<30 kW/m^2) due to the existence of the subcooling temperature with a maximum of 3 ℃ at the channel inlet for all working conditions. Regime II: the two-phase flow boiling regime under higher heat flux (q>30 kW/m^2), where phase change heat transfer occurred. The slopes of the two regimes are quite different, as indicated by the black dashed line in Fig. 2, and the transition between these two regimes is relatively abrupt, as evidenced by the kickback of the wall superheat due to the onset of nucleate boiling (ONB). In the single-phase regime, the wall superheat increased significantly with a small increase in heat flux, and forced convection dominated. In contrast, for the two-phase flow boiling regime, only a small increase in the wall superheat was observed as the heat flux increased stepwise, and the corresponding slope for the two-phase regime was much larger than that for the single-phase regime. Furthermore, the superheat increased sharply as the heat flux continued to increase, indicating the onset of dryout. In addition, the mass velocity has a prominent effect on the boiling curves when the wall superheat is greater than 15 ℃. A higher mass velocity can delay the occurrence of dryout; i.e., a higher heat flux is necessary to trigger dryout. In this study, the heating process was stopped when dryout appeared to protect the test apparatus. Hence, only the dryout data near the outlet of the test channel are obtained, as shown in Fig. 2 (b).

3.2 Analysis of the Heat Transfer Characteristics

The variation of the measured local HTC with the local vapor quality in 0.5 mm and 1 mm channels are exhibited in Fig. 3 and the cases with mass velocities of 1000 kg/m^{2}s and heat fluxes varying from 47.7 kW/m^2 to 127.6 kW/m^2 are presented. As shown in Fig. 3 (a), the HTC in the 0.5 mm micro-channel increases significantly as the heat flux increases for a fixed vapor quality. According to Eq. (4), the local HTC is calculated as the ratio of the heat flux applied to the channel to the local wall superheat. There is little change in the wall superheat in the two-phase flow boiling regime, as depicted in *Section 3.1*. Therefore, the

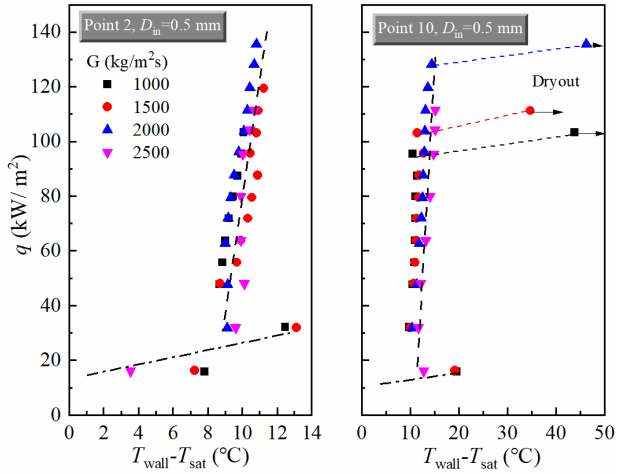

(a) (b).

Fig. 2. Boiling curves at specified locations and various mass velocities in the 0.5 mm ID channel. (a) Point 2. (b) Point 10.

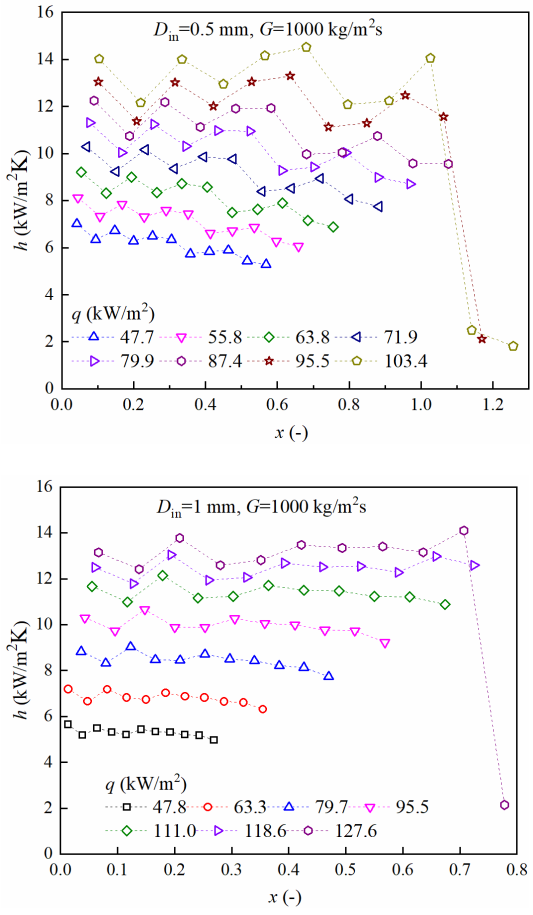

(a)

(b)

Fig. 3. Local HTC variation against the vapor quality. (a) D_{in}=0.5 mm, (b) D_{in}=1 mm.

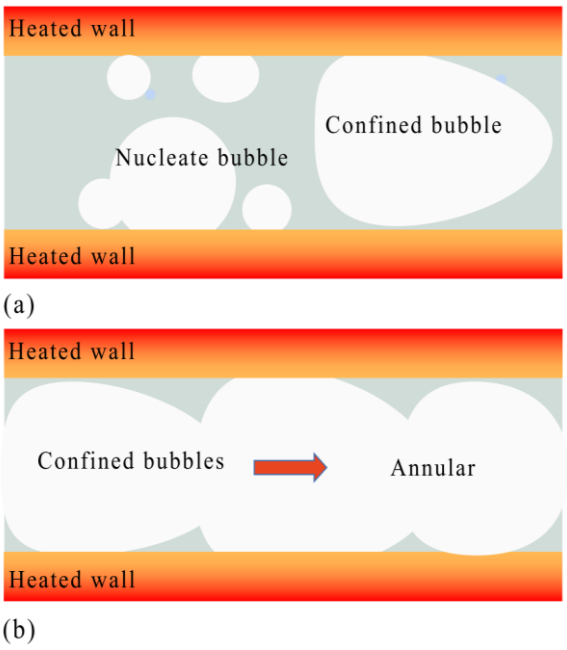

Fig. 4. The schematic diagram of the flow pattern transition in micro-channel.

heat flux applied to the channel can significantly promote the boiling heat transfer in the micro-channel. In addition, the increasing heat flux activates more nucleation points on the channel wall, and more liquid refrigerant is required for evaporation to dissipate the heat. Consequently, the vapor quality at a fixed measurement point on the channel gradually increases. However, as the vapor quality increases, the local HTC decreases slightly when the heat flux remains constant. For example, the maximum reduction in HTC is 1.69 kW/m^{2}K when q=47.7 kW/m^2. The trends of the HTC for different heat fluxes are similar, but the fluctuation of the HTC under high heat flux conditions is more evident than that under low heat flux conditions.

Previous studies on the flow boiling in micro-channels have shown that three typical flow patterns can be captured: bubbly flow, confined and elongated bubbly flow and annular flow (Yin & Jia, 2016, Yin et al.; 2014). In the present study, liquid refrigerant was pumped into the micro-channel with a small subcooling temperature of less than 3 ℃ and the refrigerant under subcooling condition was heated to the saturation condition. Bubbles were generated at the nucleation point when the vapor quality was low, usually before the first measurement point on the test channel. As the local vapor quality increased along the flow direction, the small bubbles grew or coalesced into larger ones, and the bubbles were eventually restricted by the channel wall. Consequently, the flow pattern in the micro-channel changes from bubbly flow to confined bubble flow, as shown in Fig. 4 (a). As the vapor quality further increased, the confined bubbles would elongate in the narrow channel, and the flow pattern would become annular owing to the continuous coalescence effect, as shown in Fig. 4 (b). Accordingly, the flow boiling heat transfer in the micro-channel is mainly determined by the evaporation of the liquid film between the vapor core and the heated wall, and the uneven film thickness leads to fluctuations in the local HTC. While the partial dryout of the thin liquid film during the elongated bubble and annular flows can increases the thermal resistance, leading to a slight reduction in the local HTC. When the vapor quality approached 1.0, the local HTC near the channel outlet decreases significantly because the liquid film is completely evaporated, resulting in the complete dryout at the inner channel wall and the rapid deterioration of the local HTC. For example, in Fig. 3 (a), the local HTCs for the last measuring point drop to 1.81 kW/m^{2}K when q=103.4 kW/m^2 and 2.12 kW/m^{2}K when q=95.5 kW/m^2.

As depicted in Fig. 3 (b), the trend of the local HTC in the 1 mm channel is similar to that in the 0.5 mm channel, but the fluctuation of the local HTC in the 1 mm channel is not obvious, and the dryout occurs at a smaller vapor quality when compared to that in the 0.5 mm channel. This is because the liquid velocity in the 0.5 mm channel is much higher than that in the 1 mm channel under the same mass flux, resulting in faster liquid replenishment and a better ability of the liquid to rewet the channel wall. For example, the vapor quality is about 0.7 when the dryout occurs in the 1 mm channel for q=127.6 kW/m^2, and the local HTC at the last measuring point drops to 2.15 kW/m^{2}K. In addition, it should be noted that the dryout occurs when the vapor quality is 1.0 for the ideal flow, but the velocity difference between the liquid and vapor phases induces shear stress and promotes interfacial instability for the actual flow (Martín-Callizo et al., 2008), resulting in tearing of the liquid film, thus, the dryout appears in advance.

3.3 Effect of The Mass Velocity

The local and average HTCs under identical mass velocity or heat flux are selected to indicate the effect of the mass velocity on the boiling heat transfer in the micro-channel. According to Fig. 5 (a), the local HTC profile for the 0.5 mm micro-channel at G=1000 kg/m^{2}s is similar to that at G=1500 kg/m^{2}s under the same heat flux. In addition, the local HTC is significantly improved by a higher heat flux at the same mass velocity. A similar phenomenon can also be observed in the 1 mm channel as shown in Fig. 5 (b). The average HTC versus heat flux at different mass velocities in the 1 mm channel is also collected and plotted in Fig. 5 (c). The average HTCs increase monotonically with increasing heat flux at each constant mass velocity before the occurrence of dryout. It can be concluded that the local and average HTCs are significantly enhanced by increasing the heat flux, whereas the influence of the mass velocity is minimal. The two-phase heat transfer in the micro-channel is dominated by the nucleate boiling mechanism, as indicated by this phenomenon (Lee & Lee, 2001; Bertsch et al., 2009b; Yoshida et al., 2011; Sandler et al., 2018), where the phase change mainly caused by the heat input is intense. However, it should be noted that the influence of the mass velocity on the heat transfer performance cannot be ignored in the present study because the mass velocity significantly affects the occurrence of dryout. As described in *Section 3.1*, a high heat flux is required to trigger the dryout under high mass velocity conditions hence, the heat transfer capacity of the heat exchanger depends on the mass velocity.

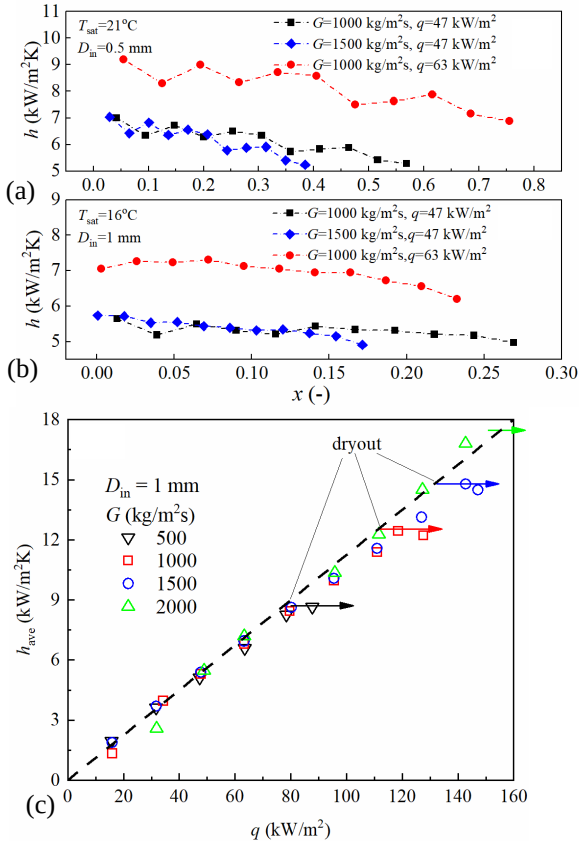

Fig. 5. Effect of the mass velocity on the HTC. (a) Local HTC in D_{in}=0.5 mm channel. (b) Local HTC in D_{in}=1 mm channel. (c) Average HTC versus heat flux in 1 mm channel.

3.4 Effect of The Inner Diameter

The variation of the average HTCs (h_{ave}) with heat fluxes in the 0.5 mm and1 mm channel are shown in Fig. 6, in which three different mass velocities are presented, respectively. In general, the average HTCs in the 0.5 mm micro-channel are slightly higher than those in the 1 mm channel under the same working conditions. The maximum increase in average HTC is approximately 22 %. This is because a smaller channel diameter generally increases the contact surface area for heat transfer and promotes more active boiling (Oh et al., 2011). Moreover, the capillary effects caused by the surface tension become prominent for the boiling heat transfer in micro-channels (Azzolin et al., 2016). As the tube diameter decreases, the thickness of the liquid film on the tube wall decreases because ofthe surface tension, resulting in lower thermal resistance and better heat transfer coefficients (Owhaib et al., 2004). The heat flux for the onset of dryout in the 0.5 mm channel is smaller than that in the 1 mm channel. The bubbles in the smaller diameter channel are more easily confined by the channel wall, and the annular flow occurs earlier. Consequently, the heat transfer performance of the smaller diameter channel at a lower mass velocity deteriorates at a lower heat flux.

3.5 Evaluation of The Heat Transfer Correlations

In this section, several existing predictive correlations of the HTC from the literature are selected for evaluation.

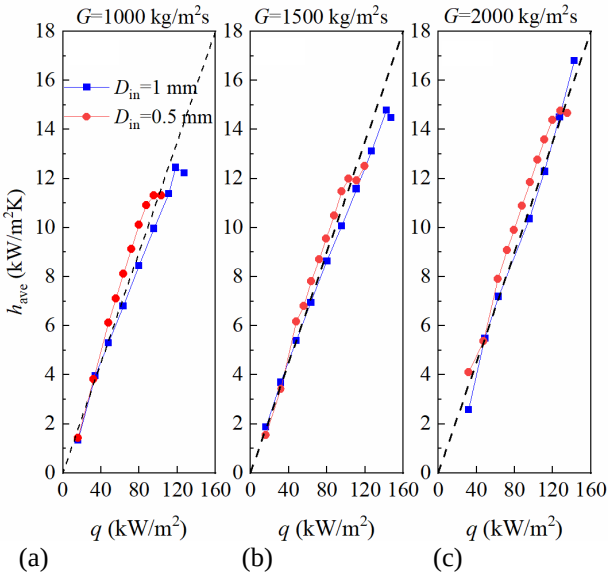

Fig. 6. Effects of micro-channel size on HTC. (a) 1000 kg/m²s; (b) 1500 kg/m²s; (c) 2000 kg/m²s.

The predicted HTCs were calculated based on the correlations and compared with the experimental values. The existing correlations can be classified into three model types: additive models (Gungor & Winterton, 1986; Liu & Winterton, 1991; Lee & Lee, 2001; Yoshida et al., 2011; Choi et al., 2007; Saitoh et al., 2007; Bertsch et al., 2009b), asymptotic models (Lee & Garimella, 2008; Kim & Mudawar, 2013a), and Nusselt-type models (Tran et al., 1996; Lee & Mudawar, 2005). In the additive model, the HTC was calculated as the sum of the convective and nucleate-boiling components. The enhancement factor F and suppression factor S were proposed to evaluate the weight factors of these two mechanisms. The function of the additive model can be expressed as $h_{tp}=Fh_{conv}+Sh_{nb}$. The asymptotic model was a modified version of the additive model with an asymptotic function that takes the form $h_{tp} = [(h_{nb}S)^n+(h_{conv}F)^n)]^{1/n}$. For the Nusselt-type models, the HTC was usually described as a power function of several dimensionless numbers (*Re*, *Bo*, *Pr*, etc.) and empirical parameters (D_{in}, x, λ, etc.).

Figure 7 exhibits the comparison of the experimental HTC with nine existing correlations in the previous studies. Three typical experimental results for the two micro-channels are shown in Fig. 7 (a) and 7 (b). It can be observed that there exist relatively large differences between the experimental and the predicted HTCs. Most of the predicted values either increase gradually or remain almost constant with the vapor quality, except for the correlation of Lee and Lee (2001), where a slight decrease in the HTC is observed in the low vapor quality region. The correlation of Kim and Mudawar (2013a) shares an almost identical trend with the experimental HTC before the occurrence of dryout, however, the predicted value is larger. Although the pre-dryout HTC data fall within the predicted range, none of the nine correlations are suitable for the accurate prediction of the experimental HTC. It should be noted that these correlations originate from the conventional size channel. Nucleate and convective boiling and/or the competition between them are the dominant mechanisms of the flow boiling heat transfer.

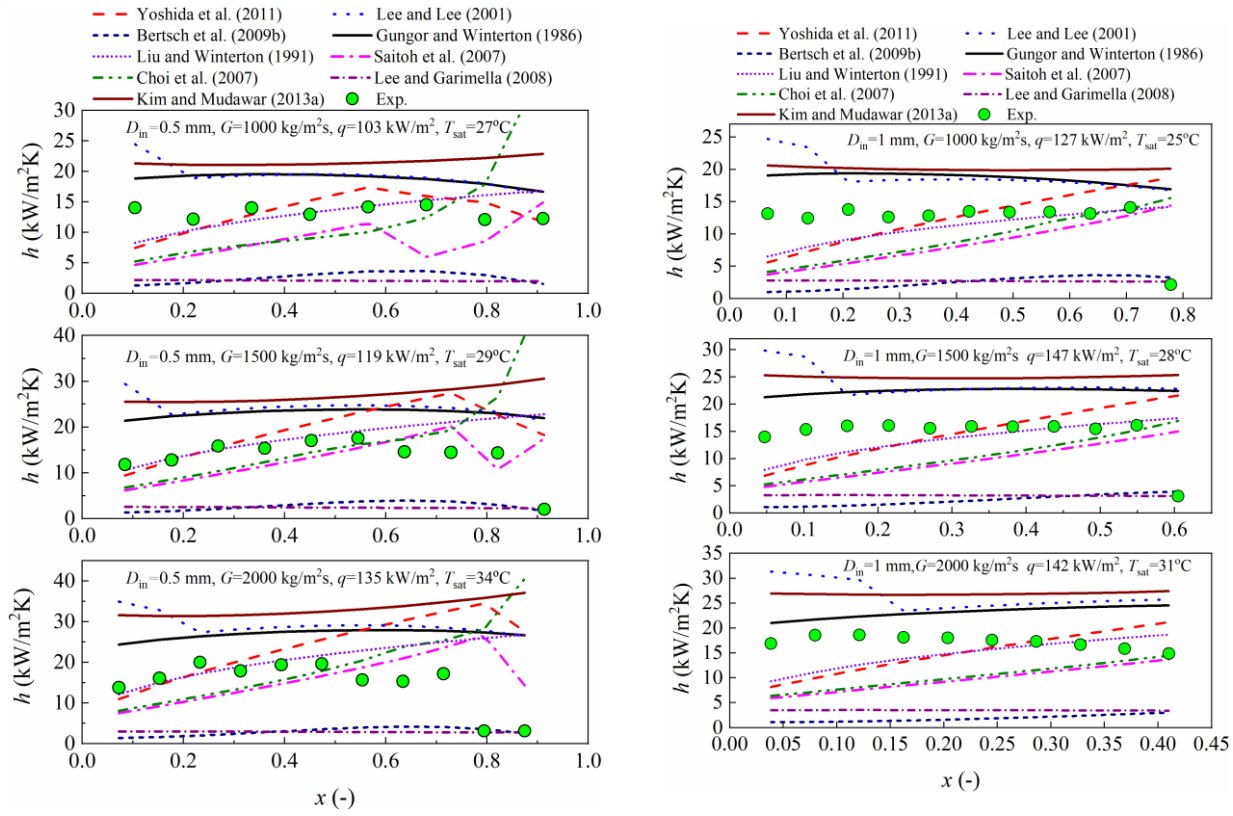

Fig. 7. Comparison of the experimental HTCs with correlations. (a) for local HTCs in D_{in}=0.5 mm channel, (b) for local HTCs in D_{in}=1 mm channel.

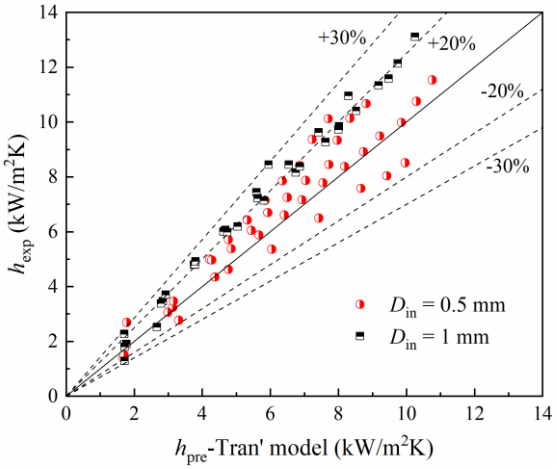

Fig. 8. Comparison of the average HTCs with the predicted results by Tran et al. (1996).

Bubbles in the conventional channel are not easily confined by the channel wall, thus, a broad transition exists between these two mechanisms. However, in the micro-channels, the nucleate bubbles are easily confined by the channel wall, and the transition of the flow pattern from bubbly flow to confined bubble flow, or even annular flow, is rapid.

As mentioned above, the average HTCs were strongly influenced by the heat flux, whereas the contribution of the mass velocity was inconspicuous. The dominant mechanism of the two-phase heat transfer is nucleate boiling. Therefore, we employed the nucleation-dominant correlation introduced by Tran et al. (1996) to predict the HTC. This correlation is expressed as follows:

$$h_{tp} = 8.4\times10^{-5}\left(Bo^2We_l\right)^{0.3}\left(\rho_l/\rho_v\right)^{-0.4} \tag{7}$$

It should be noticed that the heat transfer model proposed by Tran et al. (1996) was developed from the collected pre-dryout database in small channels. Therefore, the experimental data for dryout were excluded. The comparison of the experimental average HTCs and predicted HTCs calculated using Tran's model is shown in Fig. 8. The percentage of the data falling within the ±30 % and the ±20 % error bands are considered for the evaluation. As shown in Fig. 8, the data in the 1 mm channel are slightly underestimated. There are 97.62 % and 96.97 % of the data for the 0.5 mm and the 1 mm micro-channel fall within the ±30 % error band, respectively. More precisely, there are 90.47 % and 51.52 % of the data for the 0.5 mm and the 1 mm micro-channel, respectively, fall within the ±20 % error band.

3.6 Pressure Drop Characteristics and Evaluation of the Correlations

The frictional pressure drop is important for the safe operation of microscale heat exchangers. The total pressure drop was determined as the difference between the pressures measured by the pressure sensors at the inlet and outlet of the micro-channels. The total pressure drop includes gravitational ($\Delta p_{tp,g}$), accelerational ($\Delta p_{tp,a}$) and frictional ($\Delta p_{tp,fric}$) components:

$$\Delta p_{tp,total} = \Delta p_{tp,g} + \Delta p_{tp,a} + \Delta p_{tp,fric} \tag{8}$$

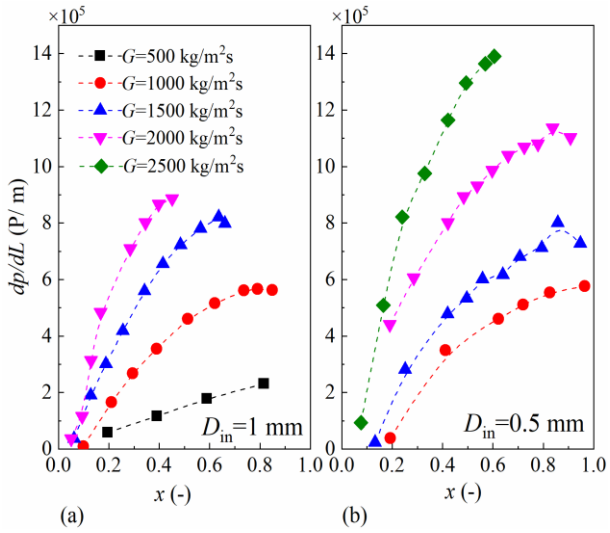

Fig. 9. The variation of FPD gradient versus vapor quality in (a) D_{in}=1 mm micro-channel and (b) D_{in}=0.5 mm micro-channel.

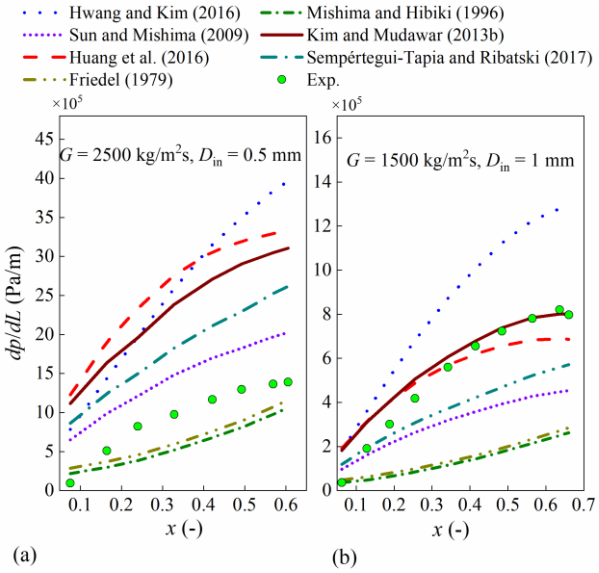

Fig. 10. Comparison of the experimental FPD with predictive models from the literature. (a) G=2500 kg/m^{2}s, D_{in}=0.5 mm. (b) G=1500 kg/m^{2}s, D_{in}=1 mm.

The gravitational pressure drop in the horizontal channel is 0. The acceleration pressure drop is calculated using the following formula:

$$\Delta p_{\mathrm{tp,a}} = G^2 \left\{ \begin{array}{l} \left(\dfrac{x^2}{\rho_{\mathrm{v}}\varepsilon} + \dfrac{(1-x)^2}{\rho_{\mathrm{l}}(1-\varepsilon)} \right)_{\mathrm{out}} \\ -\left(\dfrac{x^2}{\rho_{\mathrm{v}}\varepsilon} + \dfrac{(1-x)^2}{\rho_{\mathrm{l}}(1-\varepsilon)} \right)_{\mathrm{in}} \end{array} \right\} \tag{9}$$

where ε denotes the void fraction, which is calculated by the revised correlation of Rouhani and Axelsson (1970) suggested by Steiner (1993):

$$\varepsilon = \frac{x}{\rho_{\mathrm{v}}} \left(\begin{array}{l} \left(1+0.12(1-x)\right)\left(\dfrac{x}{\rho_{\mathrm{v}}} + \dfrac{1-x}{\rho_{\mathrm{l}}} \right) \\ + \dfrac{1.18(1-x)\left(g\sigma\left(\rho_{\mathrm{l}}-\rho_{\mathrm{v}}\right)/\rho_{\mathrm{l}}^2\right)^{0.25}}{G} \end{array} \right)^{-1}. \tag{10}$$

The FPD gradient for flow boiling is depicted as:

$$\left(\frac{dp}{dz}\right)_{\mathrm{tp,fric}} = \frac{\Delta p_{\mathrm{tp,total}} - \Delta p_{\mathrm{tp,a}}}{L} \tag{11}$$

The two-phase FPD gradient versus vapor quality under various operating conditions is shown in Fig. 9. The FPD gradient increases with an increase in mass velocity and vapor quality. In addition, the FPD gradient in the 0.5 mm ID channel is higher than that in the 1 mm ID channel under similar experimental conditions. A higher mass velocity and smaller channel size lead to an increase in the fluid velocity, consequently, the contribution of the shear stress between the fluid and the channel wall to the FPD increases. Meanwhile, the different velocities between the liquid and vapor phases at high vapor quality promote the interfacial shear stress, which also increases the FPD in the micro-channel. For the test channel with D_{in}=0.5 mm, the FPD decreases slightly at x > 0.9, owing to the occurrence of dryout at the channel outlet. A similar trend was reported by Xu et al. (2016).

Lockhart and Martinelli (1949) developed an empirical correlation by proposing the two-phase frictional multiplier for calculating the flow boiling FPD in channel.

$$\left(\frac{dp}{dz}\right)_{\mathrm{tp}} = \phi_{\mathrm{l}}^2 \left(\frac{dp}{dz}\right)_{\mathrm{l}} = \phi_{\mathrm{v}}^2 \left(\frac{dp}{dz}\right)_{\mathrm{v}} \tag{12}$$

where ϕ_l^2 and ϕ_v^2 represent the two-phase frictional multiplier:

$$\phi_{\mathrm{l}}^2 = 1 + \frac{C}{X} + \frac{1}{X^2} \tag{13}$$

$$\phi_{\mathrm{v}}^2 = 1 + CX + X^2 \tag{14}$$

where C represents the Chisholm parameter determined by the experimental conditions and the thermophysical properties of the working fluid. X represents the Martinelli parameter.

$$X^2 = \left(\frac{dp}{dz}\right)_{\mathrm{l}} \Big/ \left(\frac{dp}{dz}\right)_{\mathrm{v}} \tag{15}$$

where $(dp/dz)_l$ and $(dp/dz)_v$ are the FPD gradients of the liquid and vapor phase flows, respectively.

$$\left(\frac{dp}{dz}\right)_{\mathrm{l}} = f_{\mathrm{l}} \frac{2G^2(1-x)^2}{D_{\mathrm{in}}\rho_{\mathrm{l}}} \tag{16}$$

$$\left(\frac{dp}{dz}\right)_{\mathrm{v}} = f_{\mathrm{v}} \frac{2G^2x^2}{D_{\mathrm{in}}\rho_{\mathrm{v}}} \tag{17}$$

Based on the above basic mathematical forms, many researchers have conducted studies on the correlations for predicting the experimental FPD (Friedel, 1979; Mishima & Hibiki, 1996; Hwang & Kim, 2006; Sun & Mishima, 2009; Kim & Mudawar, 2013b; Huang et al., 2016; Sempértegui-Tapia & Ribatski, 2017). The experimental data and predicted results of the FPD gradient versus vapor quality are compared, as illustrated in Fig. 10. For

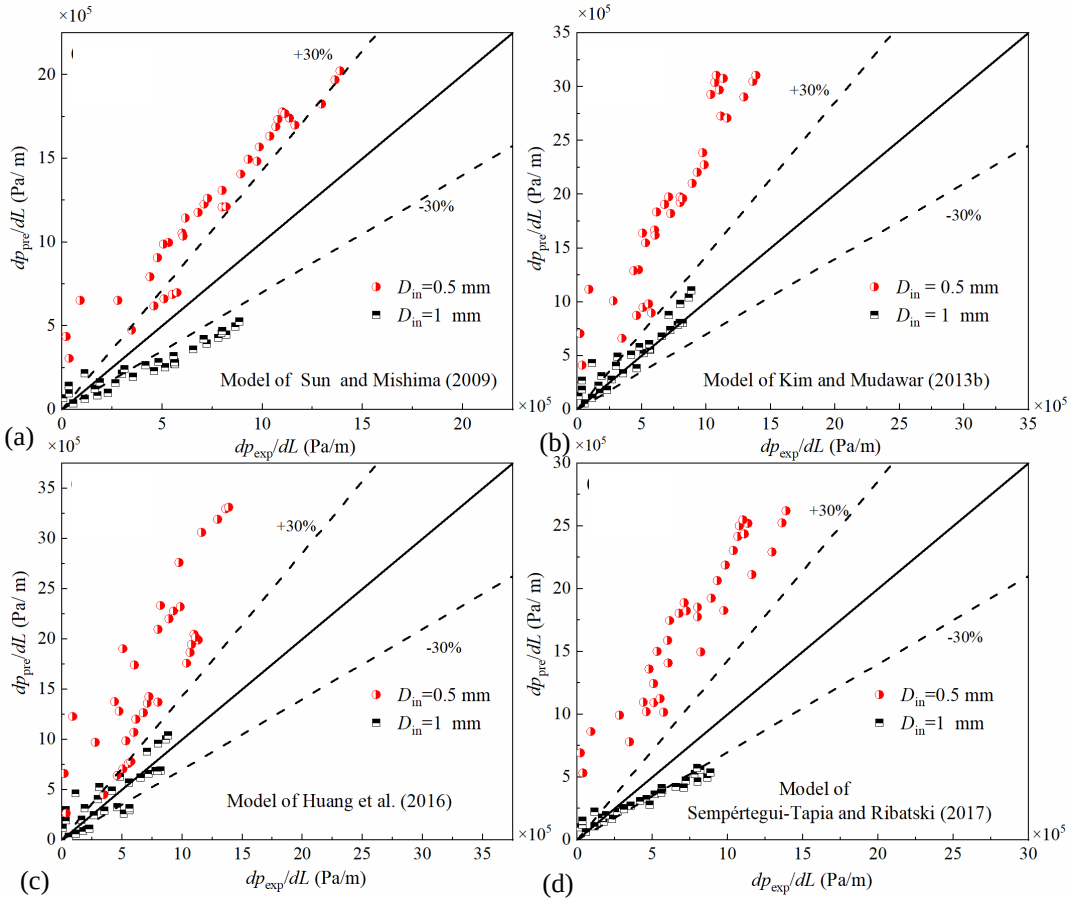

Fig. 11. Experimental FPD versus predicted results using available correlations.

the 0.5 mm channel, the correlations generally overestimate the experimental FPD, except for the correlations of Mishima and Hibiki (1996) and Friedel (1979). For the 1 mm channel, the correlations underestimate the experimental FPD, in addition to the correlation of Hwang and Kim (2006). The correlations of Sun and Mishima (2009), Kim and Mudawar (2013b), Huang et al. (2016), and Sempértegui-Tapia and Ribatski (2017) show a similar tendency to the experimental results, but the prediction accuracies of these correlations are unsatisfactory. Finally, all the experimental FPDs in the two micro-channels are compared with the values predicted by the four selected correlations (Sun & Mishima, 2009; Kim & Mudawar, 2013b; Huang et al., 2016; Sempértegui-Tapia & Ribatski, 2017) as shown in Fig. 11. There is better agreement for the results of the 1 mm channel in comparison to those of the 0.5 mm channel, and the frictional pressure drop gradients for the 0.5 mm channel are always overestimated by these correlations. The correlation of Kim and Mudawar (2013b) provides relatively good agreement for the FPD in the 1 mm micro-channel.

4. CONCLUSIONS

The flow boiling characteristics of R-134a in micro-channels were studied experimentally at mass velocities ranging from 500 kg/m^{2}s to 2500 kg/m^{2}s and heat fluxes ranging from 15 to 147 kW/m^2. The main conclusions of this study are summarized below.

The boiling curves comprised of two regimes: the single-phase regime when the heat flux is low and the two-phase flow boiling regime when the heat flux is high and phase change heat transfer occurs. The transition between these two regimes indicates the ONB.

The HTC was strongly influenced by the heat flux, and the effect of mass velocity was insignificant. Nucleate boiling is considered as the main heat transfer mechanism for R-134a flow boiling in micro-channels. The HTC in the 0.5 mm micro-channel was slightly higher than that in the 1 mm channel. The maximum increase in the average HTC was approximately 22 %.

Ten existing prediction correlations for the HTC were evaluated, and the nucleation-dominated correlation proposed by Tran et al. (1996) predicted the experimental database with relatively good accuracy.

The FPD gradient increased with an increase in the mass velocity and vapor quality, but it decreased as the channel size increase.

Seven FPD correlations from the literature were evaluated by comparing them with the experimental FPD, and the FPD gradients in the 1 mm ID channel were more consistent with the correlation developed by Kim and Mudawar (2013b).

ACKNOWLEDGEMENTS

This work was supported by the National Natural Science Foundation of China [Grant No. 52006030]; the

Shanghai Sailing Program [Grant No. 18YF1400700]; the China Postdoctoral Science Foundation [Grant No. 2018M641891]; the Fundamental Research Funds for the Central Universities of China [Grant No. 2232018D3-37].

CONFLICT OF INTEREST

The authors declare that they have no competing interests.

AUTHORS CONTRIBUTION

Longlong Feng: Methodology, Investigation, Formal analysis, Validation, Writing Writing-review & editing. Chuanchao Cao: Methodology, Investigation, Writing-original draft. Ke Zhong: Supervision, Funding acquisition. Hongwei Jia: Project administration, Supervision, Funding acquisition, Writing-review & editing.

REFERENCES

Azzolin, M., Bortolin, S., & Del Col, D. (2016). Flow boiling heat transfer of a zeotropic binary mixture of new refrigerants inside a single microchannel. *International Journal of Thermal Sciences,* 110, 83-95. https://doi.org/10.1016/j.ijthermalsci.2016.06.026

Bertsch, S. S., Groll, E. A., & Garimella, S. V. (2009a). Effects of heat flux, mass flux, vapor quality, and saturation temperature on flow boiling heat transfer in microchannels. *International Journal of Multiphase Flow,* 35(2), 142-154. https://doi.org/10.1016/j.ijmultiphaseflow.2008.10.004

Bertsch, S. S., Groll, E. A., & Garimella, S. V. (2009b). A composite heat transfer correlation for saturated flow boiling in small channels. *International Journal of Heat and Mass Transfer,* 52, 2110-2118. https://doi.org/10.1016/j.ijheatmasstransfer.2008.10.022

Chen, C. A., Li, K. W., Lin, T. F., Li, W. K., & Yan, W. M. (2021). Study on heat transfer and bubble behavior inside horizontal annuli: Experimental comparison of R-134a, R–407C, and R-410A subcooled flow boiling. *Case Studies in Thermal Engineering*, 24, 100875. https://doi.org/10.1016/j.csite.2021.100875

Choi, K. I., A.S. Pamitran and J.-T. Oh (2007). Two-phase flow heat transfer of CO2 vaporization in smooth horizontal minichannels. *International Journal of Refrigeration,* 30, 767– 777. https://doi.org/10.1016/j.ijrefrig.2006.12.006

Choi, K. I., Pamitran, A. S., Oh, C. Y., & Oh, J, T. (2008). Two-phase pressure drop of R-410A in horizontal smooth minichannels. *International Journal of Refrigeration* 31(1), 119–129. https://doi.org/10.1016/j.ijrefrig.2007.06.006

Dang, C., Jia, L., Peng, Q., Yin, L. F., & Qi, Z. L. (2020). Comparative study of flow boiling heat transfer and pressure drop of HFE-7000 in continuous and segmented microchannels. *International Journal of Heat and Mass Transfer,* 148, 119038. https://doi.org/10.1016/j.ijheatmasstransfer.2019.119038

Dorao, C. A., Drewes, S., & Fernandino, M. (2018). Can the heat transfer coefficients for single-phase flow and for convective flow boiling be equivalent? *Applied Physics Letters,* 112, 064101. https://doi.org/10.1063/1.5018659

Fayyadh, E. M., Mahmoud, M. M., Sefiane, K., & Karayiannis, T. G. (2017). Flow boiling heat transfer of R134a in multi microchannels. *International Journal of Heat and Mass Transfer,* 110, 422-436. https://doi.org/10.1016/j.ijheatmasstransfer.2017.03.057

Feng, L., Zhong, K., Xiao, X., Jia, H., & Luo, X. (2022). Experimental investigation on flow boiling characteristics of HFO-1234yf in a 0.5 mm microchannel. *International Journal of Refrigeration,* 136, 71-81. https://doi.org/10.1016/j.ijrefrig.2022.01.015

Friedel, L. (1979). *Improved friction pressure drop correlation for horizontal and vertical two-phase pipe flow.* Proceedings of European Two-Phase Flow Group Meeting Ispra, Italy.

Gan. C. J., Wang, W., & Zhang, L. (1998). Influence of tube's diameter on boiling heat transfer performance in small diameter tubes. *Journal of Thermal Science,* 7, 49-53. https://doi.org/10.1007/s11630-998-0025-x

Gungor, K. E., & Winterton, R. H. S. (1986). A general correlation for flow boiling in tubes and annuli. *International Journal of Heat and Mass Transfer,* 29(3), 351-358. https://doi.org/10.1016/0017-9310(86)90205-X

Huang, H., Borhani, N., & Thome, J. R. (2016) Experimental investigation on flow boiling pressure drop and heat transfer of R1233zd (E) in a multi-microchannel evaporator. *International Journal of Heat and Mass Transfer,* 98, 596-610. https://doi.org/10.1016/j.ijheatmasstransfer.2016.03.051

Hwang, Y. W., & Kim, M. S. (2006). The pressure drop in microtubes and the correlation development. *International Journal of Heat and Mass Transfer,* 49(11-12), 1804-1812. https://doi.org/10.1016/j.ijheatmasstransfer.2005.10.040

Kaew-On, J., Sakamatapan, K., & Wongwises, S. (2011). Flow boiling heat transfer of R134a in the multiport minichannel heat exchangers. *Experimental Thermal and Fluid Science,* 35(2), 364-374. https://doi.org/10.1016/j.expthermflusci.2010.10.007

Kanizawa, F. T., Tibiriçá, C. B., & Ribatski, G. (2016). Heat transfer during convective boiling inside microchannels. *International Journal of Heat and Mass Transfer,* 93, 566-583. https://doi.org/10.1016/j.ijheatmasstransfer.2015.09.

083

Kew, P. A., & Cornwell, K. (1997). Correlations for the prediction of boiling heat transfer in small-diameter channels. *Applied Thermal Engineering,* 17(8), 705-715. https://doi.org/10.1016/S1359-4311(96)00071-3

Kim, S. M., & Mudawar, I. (2013a). Universal approach to predicting saturated flow boiling heat transfer in mini/micro-channels–Part II. Two-phase heat transfer coefficient. *International Journal of Heat and Mass Transfer,* 64, 1239-1256. https://doi.org/10.1016/j.ijheatmasstransfer.2013.04.014

Kim, S. M., & Mudawar, I. (2013b). Universal approach to predicting two-phase frictional pressure drop for mini/micro-channel saturated flow boiling. *International Journal of Heat and Mass Transfer,* 58(1-2), 718-734. https://doi.org/10.1016/j.ijheatmasstransfer.2012.11.045

Lee, H. J., & Lee, S. Y. (2001). Heat transfer correlation for boiling flows in small rectangular horizontal channels with low aspect ratios. *International Journal of Multiphase Flow,* 27(12), 2043-2062. https://doi.org/10.1016/S0301-9322(01)00054-4

Lee, J., & Mudawar, I. (2005). Two-phase flow in high-heat-flux micro-channel heat sink for refrigeration cooling applications: Part II—heat transfer characteristics. *International Journal of Heat and Mass Transfer,* 48(5), 941-955. https://doi.org/10.1016/j.ijheatmasstransfer.2004.09.019

Lee, P. S., & Garimella, S. V. (2008). Saturated flow boiling heat transfer and pressure drop in silicon microchannel arrays. *International Journal of Heat and Mass Transfer,* 51(3-4), 789-806. https://doi.org/10.1016/j.ijheatmasstransfer.2007.04.019

Liu, Z., & R. Winterton, H. S. (1991). A general correlation for saturated and subcooled flow boiling in tubes and annuli, based on a nucleate pool boiling equation. *International Journal of Heat and Mass Transfer,* 34 (11), 2759-2766. https://doi.org/10.1016/0017-9310(91)90234-6

Lockhart, R. W., & Martinelli, R. C. (1949). Proposed correlation of data for isothermal two-phase, two-component flow in pipes. *Chemical. Engineering and Processing*, 45, 39-48.

Martín-Callizo, C., Ali, R., & Palm, B. (2008). *Dryout incipience and critical heat flux in saturated flow boiling of refrigerants in a vertical uniformly heated microchannel.* ASME 2008 6th International Conference on Nanochannels, Microchannels, and Minichannels.

Mishima, K., & Hibiki, T. (1996). Some characteristics of air-water two-phase flow in small diameter vertical tubes. I*nternational Journal of Multiphase Flow* 22(4), 703-712. https://doi.org/10.1016/0301-9322(96)00010-9

Moffat, R. J. (1988). Describing the uncertainties in experimental results, *Experimental Thermal and Fluid Science*, 1, 3-17. https://doi.org/10.1016/0894-1777(88)90043-X

Oh, J. T., Pamitran, A. S., Choi, K. I., & Hrnjak, P. (2011). Experimental investigation on two-phase flow boiling heat transfer of five refrigerants in horizontal small tubes of 0.5, 1.5 and 3.0mm inner diameters. *International Journal of Heat and Mass Transfer*, 54(9), 2080-2088. https://doi.org/10.1016/j.ijheatmasstransfer.2010.12.021

Owhaib, W., Martin-Callizo, C., & Palm, B. (2004). Evaporative heat transfer in vertical circular microchannels, *Applied Thermal Engineering*, 24, 1241–1253. https://doi.org/10.1016/j.applthermaleng.2003.12.030

Qiu, J., Zhao, Q., Lu, M., Zhou, J., Hu, D., Qin, H., & Chen, X. (2022). Experimental study of flow boiling heat transfer and pressure drop in stepped oblique-finned microchannel heat sink. *Case Study in Thermal Engineering,* 30, 101745. https://doi.org/10.1016/j.csite.2021.101745

Rouhani, S. Z., & Axelsson, E. (1970). Calculation of void volume fraction in the subcooled and quality boiling regions. *International Journal of Heat and Mass Transfer*, 13, 383-393. https://doi.org/10.1016/0017-9310(70)90114-6

Saisorn, S., Kaew-On, J., & Wongwises, S. (2011). Two-phase flow of R-134a refrigerant during flow boiling through a horizontal circular mini-channel. *Experimental Thermal and Fluid Science,* 35(6), 887-895. https://doi.org/10.1016/j.expthermflusci.2011.01.008

Saitoh, S., Daiguji, H., & Hihara, E. (2005). Effect of tube diameter on boiling heat transfer of R-134a in horizontal small-diameter tubes. *International Journal of Heat and Mass Transfer,* 48(23), 4973-4984. https://doi.org/10.1016/j.ijheatmasstransfer.2005.03.035

Saitoh, S., Daiguji, H., & Hihara, E. (2007). Correlation for boiling heat transfer ofR-134a in horizontal tubes including effect of tube diameter. *International Journal of Heat and Mass Transfer*, 50, 5215–5225. https://doi.org/10.1016/j.ijheatmasstransfer.2007.06.019

Sandler, S., Zajaczkowski, B., & Krolicki, Z. (2018). Review on flow boiling of refrigerants R236fa and R245fa in mini and micro channels. *International Journal of Heat and Mass Transfer,* 126, 591-617. https://doi.org/10.1016/j.ijheatmasstransfer.2018.05.048

Sempértegui-Tapia, D. F., & Ribatski, G. (2017). Two-phase frictional pressure drop in horizontal micro-

scale channels: Experimental data analysis and prediction method development. *International Journal of Refrigeration,* 79, 143-163. https://doi.org/10.1016/j.ijrefrig.2017.03.024

Steiner, D. (1993). *Heat Transfer to boiling saturated liquids, in: VDI Wärmeatlas (VDI Heat Atlas).* VDI Verlag, Düsseldorf, Germany.

Sun, L., & Mishima, K. (2009). Evaluation analysis of prediction methods for two-phase flow pressure drop in mini-channels. *International Journal of Multiphase Flow,* 35(1), 47-54. https://doi.org/10.1016/j.ijmultiphaseflow.2008.08.003

Tran, T. N., Wambsganss, M. W., & France, D. M. (1996). Small circular- and rectangular- channel boiling with two refrigerants. *International Journal of Multiphase Flow*, 22(3), 485-498. https://doi.org/10.1016/0301-9322(96)00002-X

Wang, Y., & Sefiane, K. (2012). Effects of heat flux, vapour quality, channel hydraulic diameter on flow boiling heat transfer in variable aspect ratio micro-channels using transparent heating. *International Journal of Heat and Mass Transfer*, 55(9), 2235-2243. https://doi.org/10.1016/j.ijheatmasstransfer.2012.01.044

Wu, J., Koettig, T., Franke, C., Helmer, D., Eisel, T., Haug, F., & Bremer, J. (2011). Investigation of heat transfer and pressure drop of CO2 two-phase flow in a horizontal minichannel. *International Journal of Heat and Mass Transfer,* 54(9), 2154-2162. https://doi.org/10.1016/j.ijheatmasstransfer.2010.12.009

Xu, Y., Fang, X., Li, D., Li, G., Yuan, Y., & Xu, A. (2016). An experimental study of flow boiling frictional pressure drop of R134a and evaluation of existing correlations. *International Journal of Heat and Mass Transfer*, 98, 150-163. https://doi.org/10.1016/j.ijheatmasstransfer.2016.03.018

Yang, C. Y., & Webb, R. L. (1996). Friction pressure drop of R-12 in small hydraulic diameter extruded aluminum tubes with and without micro-fins. *International Journal of Heat and Mass Transfer*, 39(4), 801-809. https://doi.org/10.1016/0017-9310(95)00151-4

Yin, L. F., & Jia, L. (2016). Confined bubble growth and heat transfer characteristics during flow boiling in microchannel. *International Journal of Heat and Mass Transfer,* 98, 114-123. https://doi.org/10.1016/j.ijheatmasstransfer.2016.02.063

Yin, L. F., Jia, L., Guan, P., & Liu, D. (2014). Experimental investigation on bubble confinement and elongation in microchannel flow boiling. *Experimental Thermal and Fluid Science*, 54, 290-296. https://doi.org/10.1016/j.expthermflusci.2014.01.004

Yoshida, S., Mori, H., Hong, H., & Matsunaga, T. (2011). Prediction of Heat Transfer Coefficient for Refrigerants Flowing in Horizontal Evaporator Tubes. *Transactions of the Japan Society of Refrigerating and Air Conditioning Engineers*.